The Gut-Brain Axis: Exploring the Role of the Gut Microbiome in Pathogen Avoidance Behaviors in *C. elegans*

WPI

A Major Qualifying Project Report submitted to the Faculty of
Worcester Polytechnic Institute
in the partial fulfillment of the Degree of Bachelor of Science
in
Biology and Biotechnology

Submitted by:
Alexis Wood

Submitted to:
Dr. Reeta Prusty Rao

This report represents the work of one WPI Undergraduate Student submitted to the faculty as evidence of completion of a degree requirement. WPI routinely publishes these reports on its website without editorial or peer review.

Abstract

The gastrointestinal tract harbors a diverse microbial community, collectively referred to as the gut microbiome. Interconnected via neural, endocrine, and immune pathways, the gut serves as a vital component of physiological homeostasis. The composition of the gut microbiome profoundly influences the body's responsiveness to external stimuli, implicating gut dysbiosis in various diseases, including irritable bowel syndrome (IBS) and depression.

Current research endeavors aim to elucidate the intricate dynamics of the gut-brain axis in disease pathogenesis and prevention, utilizing animal models to manipulate gut-brain pathways. In this particular investigation, the immune system of *C. elegans* was modulated through pathogen exposure to investigate the role of the gut-brain axis in mediating behavioral responses to environmental cues.

To dissect the genetic underpinnings of these behaviors, *C. elegans* were subjected to *C. albicans* infection for either two or four hours and the expression of five immune-related genes was targeted via quantitative polymerase chain reaction (qPCR). Notably, *daf7, pmk1, flp21,* and *npr1* were upregulated in response to four hours of pathogen exposure. These findings underscore the intertwined roles of genetics and microbiome composition in modulating immune responses through the gut-brain axis in the face of environmental stimuli.

Given the structural similarities between *C. elegans* and the human body, these results carry significant implications for future investigations into human health and disease.

Acknowledgments

This endeavor would not have been possible without the guidance of my advisor, Dr. Reeta Prusty Rao, and mentor, Dr. Romina Elisa D'Almeida. Thank you Dr. Rao for entrusting me in your laboratory and providing me with the space and resources to gain invaluable experience in biotechnology. Thank you Dr. D'Almeida for your willingness to teach me and answer my questions throughout my MQP journey.

I am also grateful to WPI for the opportunity to have hands-on learning experiences and work with professionals in my chosen career field. Because of these opportunities, I feel more confident and prepared to embark on my professional career in biotechnology.

Table of Contents

List of Figures

List of Tables

Introduction

The Gut Microbiota

The microbiome is a highly diverse community of symbiotic microorganisms living on and in every animal on Earth. The gut microbiome refers to the population of microbes occupying the gastrointestinal (GI) tract, residing primarily in the colon of vertebrates (Cresci & Izzo, 2019). Although the gut microbiome is a highly pursued area of research, researchers have yet to fully understand its diversity and functional role in the human body. The human gut microbiome is predicted to house around 1,000 microbial species, totaling over 100 trillion microbial cells, which are known to influence our physiology, metabolism, nutrition, and immune system in various ways (Cresci & Izzo 2019). Disruption in this population, known as dysbiosis, has been linked to various gastrointestinal, metabolic, and neuropsychiatric diseases such as inflammatory bowel syndrome (IBS), diabetes, and major depressive disorder (MDD) (Guinane & Cotter, 2013).

The gut microbiome is primarily composed of anaerobic bacteria from the firmicutes and bacteroidetes phylum; however, viruses, eukaryotes, yeasts, and archaea are also present in small percentages. Most inhabitants of the gut are mutualistic, meaning both the host and microbes benefit mutually from close interactions with one another. Gut microbes interact with the mucosal lining of the intestines, providing the host with benefits such as epithelial cell protection, metabolic regulation, immunomodulation, nutrient absorption, and production of enzymes and short-chain fatty acids (SCFA) (Cresci & Izzo 2019). Factors such as diet, the environment, antibiotic use, infection, and stress are known to influence changes in gut microbiome composition. Such changes affect the interactions between gut microbes and the host, potentially influencing other processes or pathways that are essential to homeostasis (Chen et al., 2013).

Metagenomic and shotgun sequencing technologies have been used to characterize much of the human gut's genetic content, yet progress to determine the functional significance of these genes is challenged considerably by the vast microbial diversity across the human population. The use of germ-free (GF) and specific pathogen-free (SPF) mice, and more recently nematodes has allowed for considerable advancements in our understanding of the microbiome's function, having profound implications for human health. For example, Hills and colleagues identified decreased concentration of fecal short-chain fatty acids (SCFA)–byproducts of anaerobic fermentation–as a fecal biomarker for IBS (2019). Another study by Harrison et al found co-occurrence patterns between bacterial and fungal taxa, suggesting that host selection of interactions between bacteria and fungi may play a role in host health and disease. These discoveries, and many others, are largely attributed to studies of the gut-brain axis, a regulatory pathway to which microbes make significant contributions.

The Gut-Brain Axis

The gut-brain axis is a bidirectional communication network existing between the gut and the central nervous system that is modulated by an assembly of neural, endocrine, and immune pathways. These signaling pathways are activated by a variety of factors, including the products of microbial metabolism. Gut microbes, which inhabit the outer mucosal layer of the intestinal barrier, play a central role in gut-brain communication pathways (Chen et al., 2013). Among the most important metabolites produced by gut microbes are short-chain fatty acids (SCFA), such as butyrate, propionate, and acetate. SCFA are ligands that bind to G-protein coupled receptors on enteroendocrine cells (EECs) to stimulate the secretion of neuropeptides and hormones. SCFAs also directly influence the synthesis of neurotransmitters, such as serotonin, dopamine, and GABA, and are essential to maintaining tight junctions between intestinal epithelial cells (Cussotto et al., 2018). Structural impairment of the intestinal lining caused by stress or poor diet, for instance, results in increased gut permeability. Under these conditions, commensals and their byproducts can penetrate the barrier and interact with neuroendocrine and immune components, thereby inducing an immune response (Generoso et al., 2021).

Emerging evidence increasingly supports an association between neurologic function, behavior, and the gut-associated immune system. Overlapping manifestations of immune responses and psychiatric disorders, such as GI upset and fatigue, have raised questions as to whether the etiology of disorders like depression involves the gut microbiome. The idea of bacteria modulating human behavior and emotions, however, is a concept that has been explored previously. In 1910, Dr. George Porter Philips reported improved depressive symptoms in adults receiving a lactic acid bacteria-containing supplement (Philips JGP, 1910; Foster et al., 2017). More recently, studies in which the gut of germ-free mice was colonized with prevalent human gut bacteria have reported reversed or ameliorated anxiolytic and depressive symptoms. This growing body of knowledge–while attributed to mostly animal studies–has significant implications for the future of psychiatry and its approach to various neuropsychiatric conditions.

C. elegans as a model host for the gut-brain axis

Germ-free mice have traditionally been used to study the connections between the gut and the brain because of their ease of manipulation and resemblance to human anatomy. More recently, *Caenorhabditis elegans* has emerged as a relevant model to probe the gut-brain axis. *C. elegans* is a nematode with numerous functional counterparts in humans and a fully sequenced genome comprised of clear orthologs of genes associated with human disease (Corsi et al., 2015). In the laboratory, *C. elegans* grow optimally on nematode growth media (NGM) containing a lawn of *Escherichia coli* as their preferred food source. They undergo four larval stages (L1-L4), growing from 0.25 to 1.0 millimeters in length (as shown in **Figure 1**) in approximately 37-45 hours at 20 ℃. Under these conditions, *C. elegans* primarily exist as self-fertilizing hermaphrodites, each producing up to 300 self-progeny once fully mature.

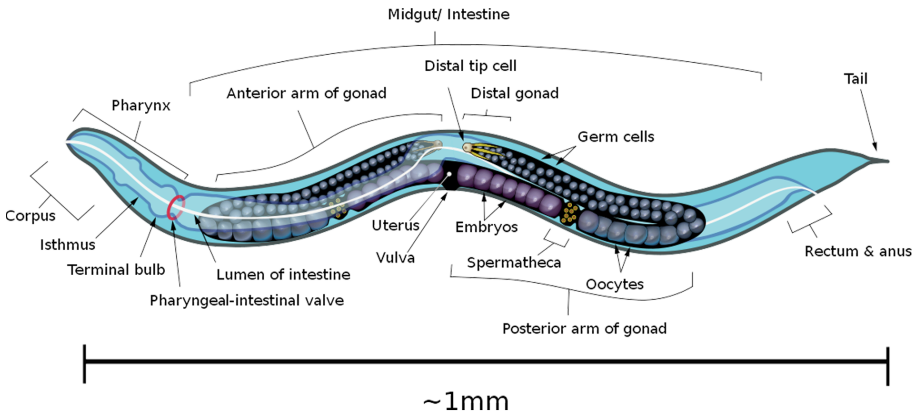

Figure 1. *Anatomical diagram of C. elegans nematode (adult hermaphrodite, L4 stage)*

C. elegans Gastrointestinal Tract

The outermost layer of C. elegans is comprised of several bands of muscle that control the movement of the organism–hence why they are referred to as a 'series of concentric circles'. The digestive, excretory, and reproductive systems are located in the neuromuscular region of the organism. The digestive system begins at the anterior side of the organism (where bacteria enter), passes through the pharynx, and ends in the intestine. The intestine is attached to the posterior pharynx and runs almost the entire length of the organism. The intestinal epithelium (the gut) houses the innate immune system, elements of which have conserved orthologs in mammals. Because *C. elegans* lacks a circulatory system or immune cells, the intestinal epithelium constitutes their primary line of defense against ingested pathogens (Corsi et al., 2015).

C. elegans Nervous System

The nervous system of adult hermaphrodites contains 302 neurons, which are localized in a few ganglia in the head, the ventral cord, and the tail. More than 7,000 chemical synapses and gap junction connections are made by the neurons in four central locations of the body: the nerve ring, the ventral nerve cord, the dorsal nerve cord, and the neuropil of the tail. Nerve conduction in *C. elegans* is primarily passive, meaning the neurons do not undergo action potentials. The neurons are, however, modulated by various neuroendocrine signals and exhibit receptors for some of the most common neurotransmitters, including acetylcholine, dopamine, serotonin, glutamate, and GABA. Chemosensory neurons in *C. elegans* express over one thousand G protein-coupled receptors that function as chemoreceptors, allowing *C. elegans* to recognize and respond to molecular cues in the environment (Corsi et al., 2015).

C. elegans utilize both sensory and motor neurons to navigate their environment and stimulate behavioral responses to harmful stimuli. The presence and quality of food in its environment, for example, regulates feeding behaviors by stimulating neurons primarily in the head and upper GI tract (*Wormatlas)*. *C. elegans* feeding depends on the actions of the pharynx, a neuromuscular tube that pumps and crushes bacteria from the environment (see **Figure 2)**. The pharyngeal

nervous system contains 20 neurons of 14 distinct anatomical classes, three of which (M3, M4, MC) are important for normal feeding behaviors. The pharyngeal nervous system is also believed to play a role in avoidance-related feeding behaviors. Shtonda and Avery in their 2006 comparative study, for example, demonstrated *C. elegans'* ability to seek out higher-quality food and to modify their feeding behaviors based on prior food encounters. This association was also demonstrated by Cook et al, in which worms with pharynx-specific mutations exhibited a lesser ability to distinguish between higher and lower-quality foods (2020).

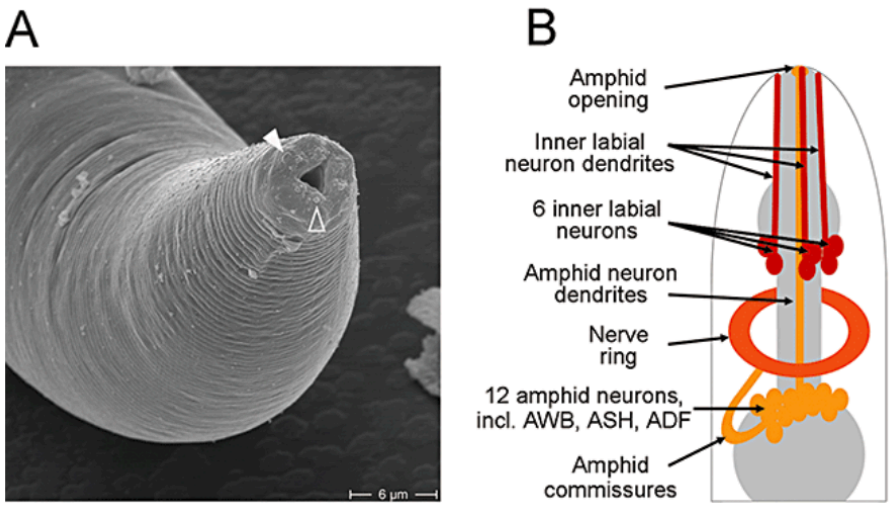

Figure 2. *(A) Depiction of C. elegans pharynx (B) The head olfactory nervous system in C. elegans*

C. elegans Behavior and Genetics

A two-choice preference assay conducted by Ha and colleagues demonstrates *C. elegans'* ability to learn avoidance behaviors in response to infection. Given the choice between OP50 and the pathogenic bacteria *Pseudomonas aeruginosa*, *C. elegans* initially exhibited attraction towards the pathogen due to its production of homoserine lactones. After a period of exposure, however, these compounds became repulsive and *C. elegans* avoided the pathogen. The researchers proposed that AWB and AWC chemosensory neurons were responsible for mediating the repulsive and attractive responses to the volatile compounds. *P. aeruginosa* also induces increased transcription of tryptophan hydroxylase (Tph-1), the rate-determining enzyme in serotonin biosynthesis, which plays a crucial role in learned olfactory preference. The researchers concluded that exposure to volatile odors produced by *P. aeruginosa* induced serotonin production in *C. elegans* ADF chemosensory neurons, resulting in learned avoidance behaviors (Meisel and Kin, 2014).

In addition to being unable to immediately distinguish food sources from pathogens, *C. elegans* lack an adaptive immune system, which enables vertebrate species to recognize and destroy harmful substances after prior exposure. The study by Ha et al, therefore, demonstrates the pertinent role of cell-to-cell communication pathways in defending *C. elegans* against infection. Enterocytes–or gut epithelial cells–are one group of cells believed to be critical in this defense

mechanism (Cook et al, 2020). Within the past decade, researchers have sought to pinpoint specific genes involved in promoting behavioral changes in response to infection. Using qPCR, researchers have identified several genes that could be associated with pathogen avoidance behaviors in *C. elegans*, including Neuropeptide receptor 1 (*npr1*), Mitogen-activated protein kinase 1 (*pmk1*), FMRF-like peptide 21 (*flp21*) and 18 (*flp18*), and Dauer Formation 7 (*daf7*).

Npr1 is a G protein-coupled receptor related to mammalian neuropeptide Y receptors that transmits stress signals when bound by neuropeptides, such as *flp18* and *flp21* (Singh & Aballey, 2019). Functions influenced by the presence of food sources, including aerotaxis, aggregation, locomotion, and pathogen avoidance behaviors are believed to be dependent on *npr1* receptor activity and its ligands. Genetic studies have indicated that *npr1* and other G-protein coupled receptors are part of a neural circuit that receives inputs from pathogens and integrates them to coordinate appropriate behavioral responses (*RCSB*). Reddy et al, for example, found that *C. elegans* expressing loss-of-function npr1 alleles exhibited enhanced susceptibility to killing by *P. aeruginosa (PA14)*. The enhanced susceptibility of *npr-1* mutants was rescued by a transgene containing wild-type copies of *npr1* (2009).

Pmk1 is a MAP kinase gene belonging to the *pmk3* operon. It functions in neuronal development and stress responses by enabling MAP kinase activity and activating transcriptional regulation. *Pmk1* is best known for its involvement in producing behavioral responses to stimuli, such as nicotine, other organisms, and inorganic substances. *Pmk1* in *C. elegans* OLL neurons has also been shown to regulate *npr1* expression (Bai et al, 2021). This has led some researchers to believe *pmk1* is required for defense against pathogens in *C. elegans.* One study conducted by Ermolaeva and Schumacher, for example, found enhanced killing by *P. aeruginosa* in *C. elegans* with a knockdown in the *tir1* gene, which normally activates *pmk1*, suggesting its importance to pathogen defense (2014).

Daf7 enables cytokine and transforming growth factor β receptor binding activity and is involved in cellular responses to organic substances and regulation of gene expression. *Daf7* also controls glucose metabolism and serotonin input in chemosensory neurons. Studies have shown that the expression of *daf7* by sensory neurons plays a putative role in mediating the avoidance of pathogens. One study, for example, showed that the detection of pathogenic secondary metabolites by ASI and ASJ neurons upregulates the expression of *daf7* through a canonical transforming growth factor β (TGF-β) signaling pathway. Furthermore, the lack-of-avoidance phenotype in *daf7* mutants was effectively reversed by expressing *daf7* in either ASI or ASJ neurons.

Project Objective

The following research sought to characterize the genetic basis of learned avoidance behaviors in *C. elegans* infected with *C. albicans*. Expression of the *npr1, pmk1, flp21, flp18,* and *daf7* genes

was targeted with qPCR in an attempt to quantify their role in modulating pathogen avoidance behaviors. Identification of these genetic markers via qPCR could provide insights into the neural and immune pathways that are mediated as a result of an impacted gut. Notable similarities in the anatomy, innate immune system, and neural circuits of *C. elegans* and mammals signify the importance of this research, as it may contribute to a deepened understanding of the human gut-brain connection and its capacity to influence health and disease.

Methodology

Media Preparation

Growth and manipulation of *C. elegans* required the preparation of several reagents, including nematode growth media (NGM), M9 buffer, yeast extract peptone dextrose (YPD), and lysogeny broth. The M9 buffer was prepared as outlined in Appendix D and stored on the bench. To prepare the NGM, the ingredients in Appendix A were combined in a large media bottle and autoclaved. Once the media had cooled slightly, it was poured into as many 60mm Petri dishes as possible, filling each dish about 1 cm high. The NGM growth plates were kept on the bench top overnight and then stored in the cold room (4 ℃) until needed to discourage contamination. YPD and LB were prepared as described in Appendices B and C, respectively. Once sterilized and cooled, 8mL of each reagent was transferred to glass vials; the LB was inoculated with a singular colony of *E. coli* (OP50) and spun for 12 hours at 30 ℃. Similarly, the YPD was inoculated with *C. albicans* (F15) and incubated at 37 ℃. YPD was added to the F15 suspension until an optical density (OD) of one was obtained. Some of the NGM plates were seeded with 30 microliters of the OP50 suspension for egg preparation (see below). Lastly, both suspensions were stored at 4 ℃ until needed.

Egg Preparation

To obtain *C. elegans* eggs, a 1 square centimeter piece of agar containing dauer larva was transferred to three partial OP50 plates (prepared in the previous step) and incubated at 20 ℃ for approximately 48 hours (or until the plates were populated with 50 to 100 eggs). The eggs were washed off the plates with M9 into 15 mL falcon tubes and centrifuged at 2500 rpm for 2 minutes. Subsequently, the supernatant was removed, leaving 2 mL in the falcon tube, to which 2 mL each of NaOH and 10% bleach were added to anesthetize the worms in the pellet. The solution was centrifuged again and the supernatant was removed, now leaving 1 mL in the falcon tube, to which 10mL of M9 was added to remove remnants of bacteria or worms from the pellet. After another 2 minutes of centrifugation, most of the supernatant was removed (leaving 300-500 microliters), resulting in a highly concentrated egg solution. 30 microliters of the egg solution were dispensed onto a triplicate of partial OP50 plates and incubated at 20 ℃ for approximately 45 hours (or until the larva reached the L4 stage).

Fungal Infection

When the worms reached the late L2 stage (approximately 24 hours), three full plates each of F15 and OP50 were prepared by dispensing 200 microliters of suspension onto the NGM plates, spreading the suspension into a thin layer across the surface of the agar, and incubating the plates overnight at 30 ℃ (~12 hours). About 21 hours later, the now L4 worms were washed off the plates into a 15 mL falcon tube with M9 buffer. The worm suspension was allowed to rest on the benchtop until a pellet formed (approximately 5 minutes), then the supernatant was removed and the pellet was resuspended in M9; this process was repeated three times total to remove remnants of OP50. 60 microliters of the worm suspension were dispensed onto the full plates and incubated at 20 ℃ for either 2 hours or 4 hours. After incubation, the infected and control worms were washed off the plates into separate falcon tubes, pelleted, and resuspended in M9 three times. The worm suspensions were then transferred to 1.5 mL Eppendorf tubes, to which 1 mL of Trizol was added to lyse the *C. elegans* cells. The samples were stored in the -80 ℃ freezer until needed.

RNA Isolation

The methodology used for RNA isolation was adapted from the mirVana™ miRNA Isolation Kit Protocol. Before beginning the isolation procedure, the RNA samples were removed from the -80-degree freezer, flash-frozen in liquid nitrogen, and thawed on a 37 ℃ heat block for five repetitions. The samples were then vortexed for five 30-second intervals. Subsequently, 200 microliters of chloroform were added to each sample, shaken vigorously for 30-60 seconds, and centrifuged at maximum speed for 5 minutes to separate the aqueous and organic phases. The aqueous (upper) phase was carefully removed and transferred to a fresh RNAse-free tube, to which 1.25 volumes of 100% ethanol was added.

The lysate-ethanol mixture was added to a filter cartridge attached to a collection tube and centrifuged at 10,000 rpm for 15 seconds to pass the mixture through the filter. After discarding the flowthrough, 700 microliters of miRNA wash solution 1 were drawn through the filter cartridge by centrifugation and the flowthrough was discarded once again. Then, 500 microliters of Wash Solution ⅔ was drawn through the filter cartridge, and the flowthrough was discarded; this step was repeated for a total of two washes. The assembly was spun again for 1 minute to remove residual fluid from the filter, then the filter was placed into a fresh collection tube, and 100 microliters of pre-heated (95 ℃) nuclease-free water was added to the filter. The assembly was spun for 20-30 seconds to elute the RNA and it was stored at -20 ℃ until further use.

cDNA Synthesis

The concentration of RNA in each sample was measured using a NanoDrop tool to ensure there was enough for cDNA preparation (100 ng-5 ug). Samples that had less than 100 ng of RNA were precipitated with ethanol and resuspended in 10uL of nuclease-free water. Subsequently,

contaminating DNA was removed from the samples using the TURBO DNA-free kit. This was done by adding the TURBO DNase buffer and TURBO DNase enzyme (an engineered version of wild-type DNase I) to the RNA and incubating it for 30 minutes. Subsequently, the DNase inactivation reagent was added to the samples, they were centrifuged, and the RNA-containing supernatant was carefully transferred to fresh tubes.

To synthesize cDNA from the RNA samples, the ProtoScript II Reverse Transcriptase enzymatic kit was used. First, the volume of each RNA sample needed to achieve 1 ug in a total volume of 10 uL was determined. The 10 uL solutions were prepared in two separate PCR tubes per RNA sample. The cDNA master mixes were prepared, using measurements based on the number of samples plus one to account for error (see Appendix E). Once everything had been added to the master mix except for the enzyme, it was divided into two tubes, one receiving the RT enzyme and the other receiving nuclease-free water. 10 uL of the master mix was then added to each sample. The half of samples receiving the no-RT master mix would serve as the negative controls. Each sample was briefly vortexed and then transferred to the thermocycler. The thermocycler was programmed to the appropriate parameters (10 minutes at 25 ℃, 120 minutes at 37 ℃, 5 minutes at 85 ℃, hold at 4℃) and run to completion. The samples were stored in the -20 ℃ freezer until further needed.

qPCR Analysis

The cDNA samples were combined with nuclease-free water in a 1:100 dilution; for greater accuracy, two successive 1:10 dilutions were performed. The primer mixes were prepared by combining equal parts of the forward and reverse primers with nuclease-free water. The master mixes–consisting of the primer mix, iTaq Sybr Green, and nuclease-free water–were prepared on ice (see Appendix F), and then all materials were transferred to a hood to set up the 96-well plate. 2 uL of each sample were loaded into their respective wells, followed by 8 uL of master mix. The plate contained duplicates of each sample with each primer, including a housekeeping gene (*cdc42*) combined with the negative controls. The layout of the plate, reaction volume (10 uL), and the reaction parameters (40 cycles of 2 minutes at 50 °C, 10 minutes at 90 ℃, 15 minutes at 95 ℃, and 1 minute at 61 ℃) were input into the qPCR software, then the reaction was run until completion. Finally, the experiment file was transferred to a flash drive and opened in Excel, where the relative quantification of each target gene was calculated from the Ct values (Appendix G).

Colonization Assay

C. elegans worms were raised to maturity on lawns of OP50. After approximately 45 hours, the mature worms were washed from the plates using M9, transferred to a full lawn of *C. albicans*, and incubated at 20 ℃ for 12 hours. A glass slide was prepared with a square piece of parafilm, from which a 1cm by 1cm window was cut using a blade. 2 to 3 infected worms were transferred

to the center of the window on the slide and anesthetized using 10 to 20 uL of sodium azide. 20 uL of agar was dispensed onto the worms and a coverslip was placed over top. This procedure was repeated once more with uninfected worms as a negative control. Both slides were analyzed under a digital microscope, observing both the anterior and posterior ends of the worms for colonization of *C. albicans*. Images of the worms were captured with the microscope and color-corrected to enhance the visibility of colonization and distinguishability of worm anatomy.

Results

qPCR Analysis

cDNA samples prepared from the RNA of *C. elegans* infected with *C. albicans* for either 2 or 4 hours were analyzed via qPCR. cDNA samples from uninfected RNA were also prepared as negative controls or calibrator samples. Expression of *daf7, pmk1, flp18, flp21,* and *npr1* was targeted using qPCR and analyzed using Microsoft Excel. Gene expression was analyzed by comparing the Ct values of the target genes to that of a housekeeping gene (*cdc42*). The Ct values were used to calculate the relative quantification (RQ) to determine whether infection time directly influenced the expression of the targeted genes.

Tables 1 and 2 contain the Cq, delta Cq, double delta Cq, and RQ values for *C. elegans daf7* after infection for 2 and 4 hours, respectively. Figure 3. compares the RQ value of *daf7* between the 2 and 4-hour samples. As can be observed, the RQ value for the 4-hour samples (48.7) is significantly higher than that of the 2-hour samples (1.8E-6). This indicates that the expression of *daf7* was greater after 4 hours than it was after 2 hours in infected *C. elegans*.

Table 1. qPCR results for daf7 target after 2-hour infection

Sample	Target	Cq (1)	Cq (2)	Cq Mean	Average	^Cq	^^Cq	RQ
OP50 1	DAF-7	15.96828		15.96828				
OP50 2	DAF-7		18.05731	18.05731	17.01279	-8.0533		
F15 1	DAF-7	22.35653		22.35653				
F15 2	DAF-7	29.6031		29.6031	25.97982	10.99777		
							19.05107	1.84101E-06

Table 2. qPCR results for daf7 target after 4-hour infection

Sample	Target	Cq (1)	Cq (2)	Cq Mean	Average	^Cq	^^Cq	RQ
OP50 1	DAF 7	32.14204	34.28266	33.21235				
OP50 2	DAF 7	32.13047	31.67979	31.90513	32.55874	-0.79662		
F15 1	DAF 7							
F15 2	DAF 7	31.33251	30.96713	31.14982	31.14982	-6.40261		
							-5.60599	48.70468

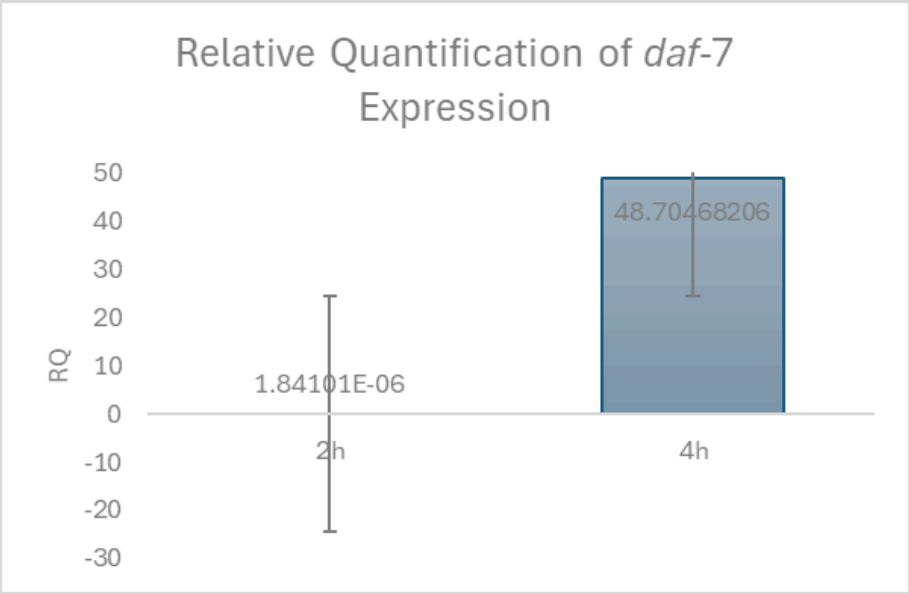

Figure 3. Relative quantification of daf7 expression by *C. elegans* infected for 2 and 4 hours with *C. albicans*. RQ values were calculated using the equations in Appendix G.

The same experimental conditions and analyses were used for the other target genes. Tables 3 and 4 contain the qPCR results and calculations for *pmk1* with 2 and 4-hour infection times, respectively. Figure 4 compares the RQ values between the two infection times. As can be observed, the RQ value for the 4-hour infection samples (102.7) was greater than that of the 2-hour infection samples (1.62E-5). These results indicate that infection of *C. elegans* with *C. albicans* for 4 hours produced a greater expression of *pmk1* than 2 hours of infection.

Table 3. Table 2. qPCR results for pmk1 target after 2-hour infection

Sample	Target	Cq (1)	Cq (2)	Cq Mean	Average	^Cq	^^Cq	RQ
OP50 1	PMK-1		21.91115	21.91115				
OP50 2	PMK-1	23.57718		23.57718	22.74417	-2.32193		
F15 1	PMK-1	18.32716	23.36601	20.84659				
F15 2	PMK-1	36.26897		36.26897	28.55778	13.57574		
							15.89766	1.63805E-05

Table 4. Table 2. qPCR results for pmk1 target after 4-hour infection

Sample	Target	Cq (1)	Cq (2)	Cq Mean	Average	^Cq	^^Cq	RQ
OP50 1	PMK 1	31.2149	31.66609	31.44049				
OP50 2	PMK 1	35.13894	34.33664	34.73779	33.08914	-0.26622		
F15 1	PMK 1		34.1557	34.1557				
F15 2	PMK 1	26.91159	27.19303	27.05231	30.604	-6.94842		
							-6.68221	102.694

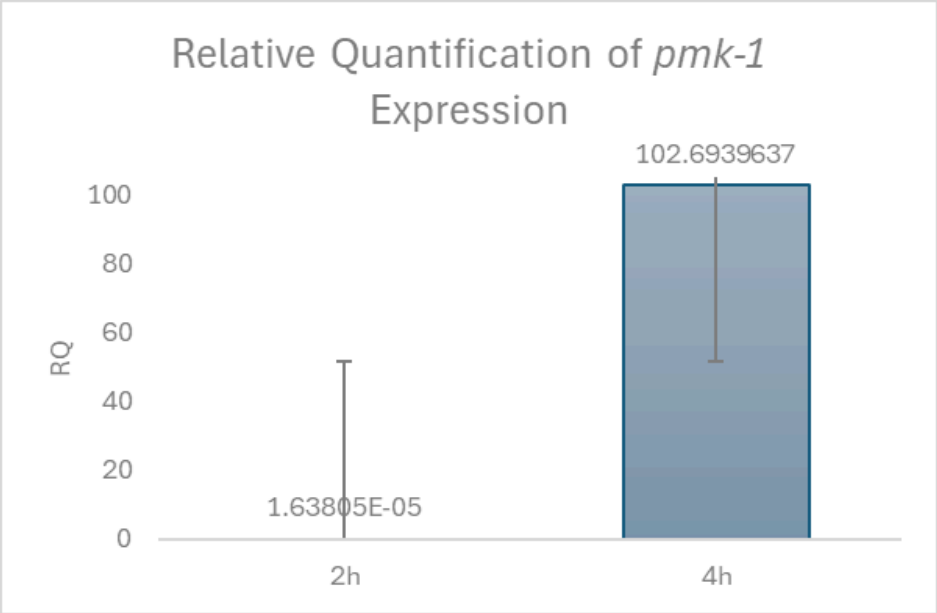

Figure 4. Relative quantification of pmk1 expression by *C. elegans* infected for 2 and 4 hours with *C. albicans*. RQ values were calculated using the equations in Appendix G.

Tables 5 and 6 and Figure 5 display the results for *flp21* expression after 2 and 4-hour infections. As can be observed in Figure 5, the RQ value for the 4-hour infection samples (28.1) was greater

than that of the 2-hour infection samples (0.001), demonstrating that longer exposure to the pathogen resulted in greater expression of the *flp21* gene by *C. elegans*.

Table 5. Table 2. qPCR results for flp21 target after 2-hour infection

Sample	Target	Cq (1)	Cq (2)	Cq Mean	Average	^Cq	^^Cq	RQ
OP50 1	FLP-21							
OP50 2	FLP 21	33.557		33.557	33.557	8.490954		
F15 1	FLP 21		38	38				
F15 2	FLP 21	28.8797	28.8695	28.8746	33.43728	18.45524		
							9.964285	0.00100104

Table 6. Table 2. qPCR results for flp21 target after 4-hour infection

Sample	Target	Cq (1)	Cq (2)	Cq Mean	Average	^Cq	^^Cq	RQ
OP50 1	FLP 21	28.334	28.4148	28.3744				
OP50 2	FLP 21	38	36.13231	37.06615	32.72028	-0.63507		
F15 1	FLP 21	33.6193		33.6193				
F15 2	FLP 21	31.79731	29.38342	30.59037	32.10481	-5.44761		
							-4.81254	28.10081

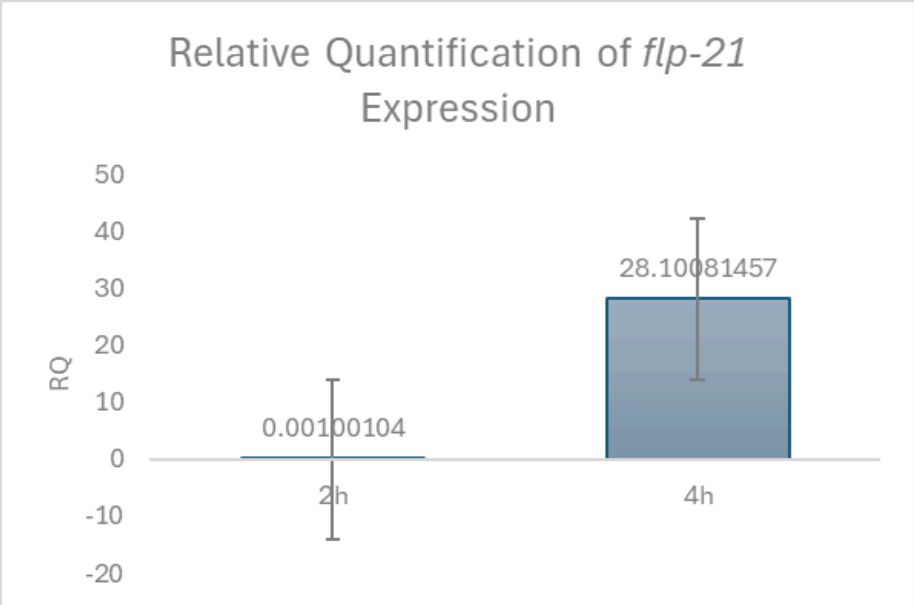

Figure 5. Relative quantification of flp21 expression by *C. elegans* infected for 2 and 4 hours with *C. albicans*. RQ values were calculated using the equations in Appendix G.

Tables 7 and 8 depict the qPCR results and analyses for *npr1* expression following 2 and 4-hour infection periods and Figure 6 compares the RQ values between these two experimental conditions. Figure 6 reveals that *npr1* expression is greater after 4 hours than it is after 2 hours of exposure to the pathogen. Of the target genes, *npr1* had the greatest expression after 2 hours but was upregulated to the least extent. After 4 hours, *npr1* expression increased by only 42 times compared to 28,072 times for *flp21*, 6,269,284 times for *pmk1*, and 26,455,413 times for *daf7*.

Table 7. Table 2. qPCR results for npr1 target after 2-hour infection

Sample	Target	Cq (1)	Cq (2)	Cq Mean	Average	^Cq	^^Cq	RQ
OP50 1	NPR-1	34.36665		34.36665				
OP50 2	NPR-1		22.16101	22.16101	28.26383	3.197739		
F15 1	NPR-1		24.98402	24.98402				
F15 2	NPR-1	22.07579		22.07579	23.52991	8.547862		
							5.350123	0.024516159

Table 8. Table 2. qPCR results for npr1 target after 4-hour infection

Sample	Target	Cq (1)	Cq (2)	Cq Mean	Average	^Cq	^^Cq	RQ
OP50 1	NPR 1	36.42697	32.9828	34.70489				
OP50 2	NPR 1	29.14203		29.14203	31.92346	-1.4319		
F15 1	NPR 1	37.27459		37.27459				
F15 2	NPR 1	34.88835		34.88835	36.08147	-1.47095		
							-0.03906	1.027441

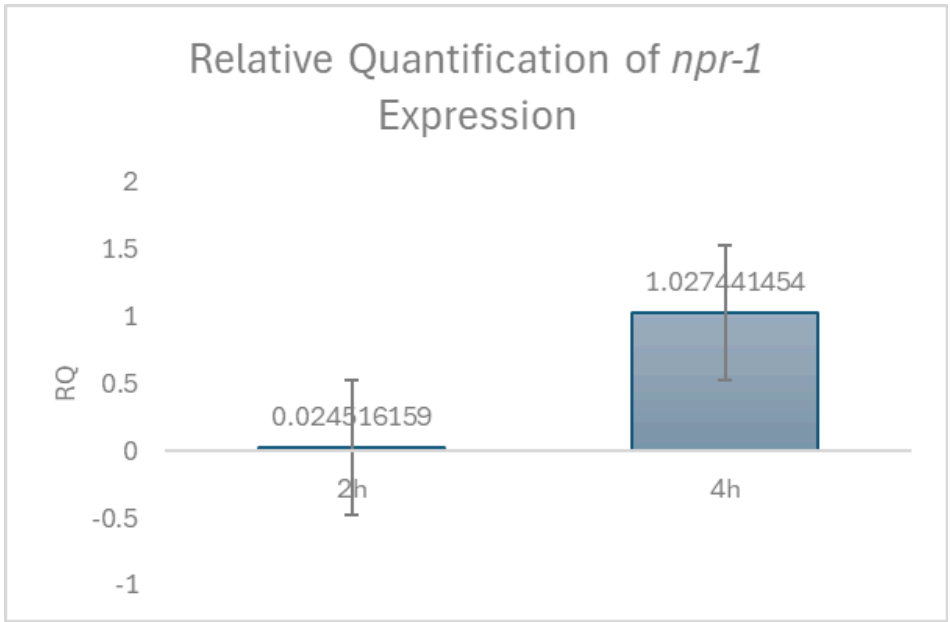

Figure 6. Relative quantification of npr1 expression by *C. elegans* infected for 2 and 4 hours with *C. albicans*. RQ values were calculated using the equations in Appendix G.

Overall, the qPCR results indicate that upregulation of *daf7, pmk1, flp21,* and *npr1* is directly influenced by infection time, as *C. elegans* exposed to *C. albicans* exhibited greater expression of these genes after 4 hours compared to only 2 hours. The data collected for the *flp18* gene was insufficient for inclusion in the RQ analysis. *Daf7* expression was upregulated to the greatest extent, followed by *pmk1, flp21,* and *npr1*. These results demonstrate the different degrees to which these genes are involved in modulating the immune system in response to pathogens in the gut.

Colonization Assay

A colonization assay was performed to observe the physiological effects of infection on *C. elegans*. Mature worms were exposed to *C. albicans* for 24 hours and then anesthetized on a glass slide. Mature worms with 24-hour exposure to *E. coli* were also used as controls. Under 400x magnification, the worm's anterior and posterior gastrointestinal tracts were visible. As seen in Figure 7, the intestine is depicted as a thin tube running from the anterior opening, through the pharynx (pointed to in Figure 7B), to the posterior side of the worm's body.

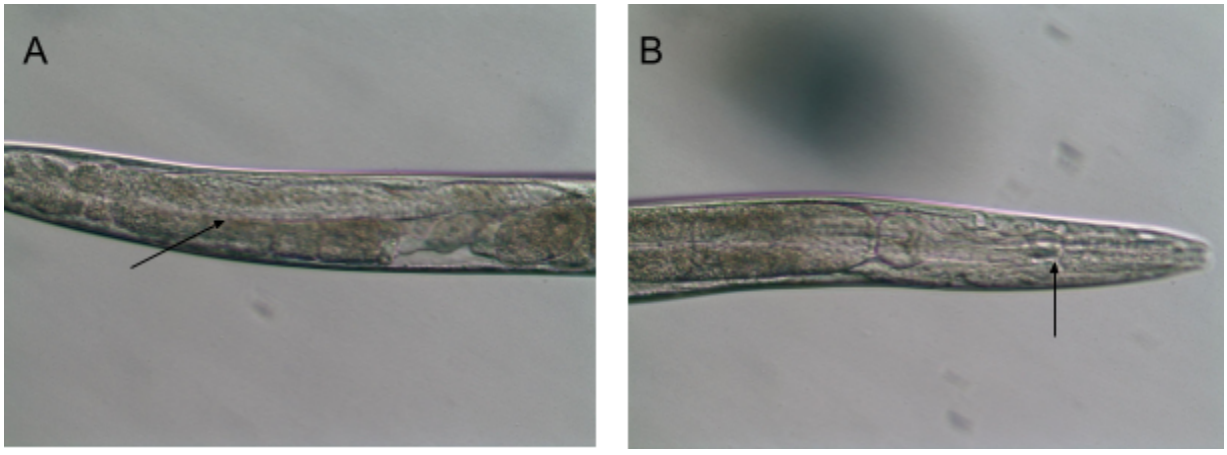

Figure 7. Anterior (A) and posterior (B) views of *C elegans* after 24-hour exposure to OP50. An arrow points to the intestine in A and the pharynx in B.

In Figure 8, the GI tract appears in the same location; however, on the anterior side, it appears thicker and deformed compared to Figure 7A. There is also noticeable colonization with *C. albicans* in the intestine and pharynx, which is likely the source of distention being observed. These results demonstrate the disruption that *C. albicans* causes to the GI tract of *C. elegans,* which is likely responsible for producing the immune responses observed in the previous analyses.

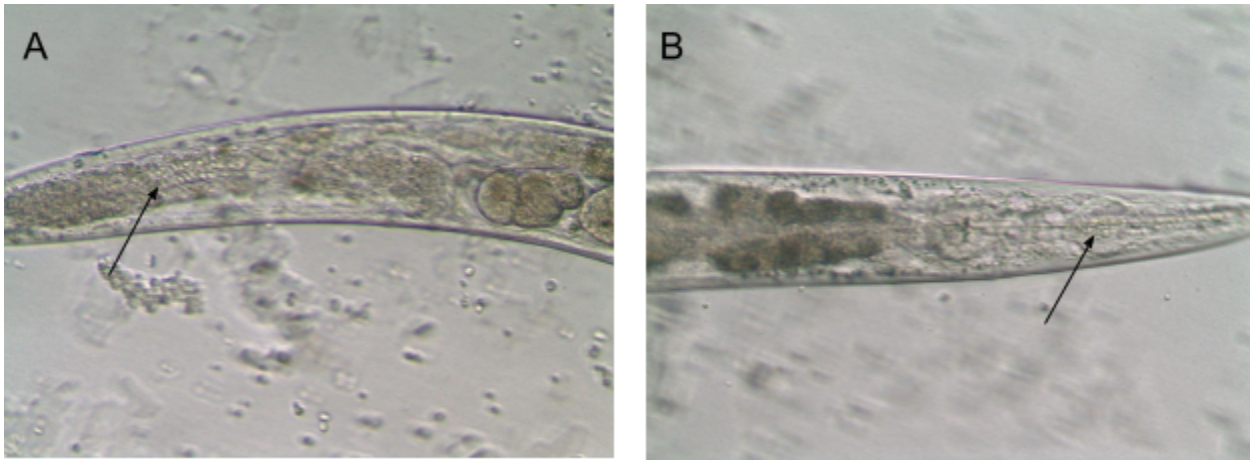

Figure 8. Anterior (A) and posterior (B) view of *C. elegans* after 24-hour candida albicans infection. Arrows in A and B point to distended, colonized portions of the intestine and pharynx, respectively.

Discussion

Previous research has identified d*af7, pmk1, flp18, flp21,* and *npr1* as key players in immune pathways associated with behavioral responses to environmental stimuli. To investigate this further, *C. elegans* were subjected to varying durations of exposure to *C. albicans* (2 and 4 hours) allowing for differential levels of infection and environmental adaptation. Subsequently, qPCR was employed to target the expression of the aforementioned genes.

It was hypothesized that the learned avoidance behaviors typically observed in *C. elegans* following prolonged exposure to pathogens would manifest as upregulation of the targeted genes in qPCR. *Daf7, pmk1, flp21,* and *npr1* were found to exhibit heightened expression levels after 4 hours of pathogen exposure compared to 2 hours of exposure, as indicated by the relative quantification (RQ) values. These results substantiate the hypothesis and suggest the involvement of these genes in facilitating behavioral immune responses via the gut-brain axis. Additionally, they implicate the gastrointestinal tract as a primary line of defense against pathogens in C. elegans.

Furthermore, the physiological effects of *C. albicans* infection, as evidenced by the colonization assay, underscore gut disturbance as a potent source of immune modulation. This discovery bears significant implications for human health. With mental and behavioral disorders becoming more prevalent, there is a pressing need for research on how lifestyle factors, such as diet and stress levels, shape the gut microbiome and its consequential impact on disease development.

A greater understanding of the interplay between microbiome components and bodily processes may help illuminate specific pathways involved in disease etiology. Such insights stand to

revolutionize research in preventive medicine and the development of targeted treatments for enigmatic diseases, including obesity and depression.

References

Bai, H., Zou, W., Zhou, W., Zhang, K., & Huang, X. (2021). Deficiency of Innate Immunity against Pseudomonas aeruginosa Enhances Behavioral Avoidance via the HECW-1/NPR-1 Module in Caenorhabditis elegans. *Infection and Immunity*, *89*(10). https://doi.org/10.1128/IAI.00067-21

Bank, R. P. D. (n.d.). *RCSB PDB - 1ALK: REACTION MECHANISM OF ALKALINE PHOSPHATASE BASED ON CRYSTAL STRUCTURES. TWO METAL ION CATALYSIS*. Www.rcsb.org. https://www.rcsb.org/structure/1alk

Bercik, P., Denou, E., Collins, J., Jackson, W., Lu, J., Jury, J., Deng, Y., Blennerhassett, P., Macri, J., McCoy, K. D., Verdu, E. F., & Collins, S. M. (2011). The Intestinal Microbiota Affect Central Levels of Brain-Derived Neurotropic Factor and Behavior in Mice. *Gastroenterology*, *141*(2), 599-609.e3. https://doi.org/10.1053/j.gastro.2011.04.052

Boulanger, R. R., & Kantrowitz, E. R. (2003). Characterization of a MonomericEscherichia coliAlkaline Phosphatase Formed upon a Single Amino Acid Substitution. *Journal of Biological Chemistry*, *278*(26), 23497–23501. https://doi.org/10.1074/jbc.m301105200

Bravo, J. A., Forsythe, P., Chew, M. V., Escaravage, E., Savignac, H. M., Dinan, T. G., Bienenstock, J., & Cryan, J. F. (2011). Ingestion of Lactobacillus strain regulates emotional behavior and central GABA receptor expression in a mouse via the vagus nerve. *Proceedings of the National Academy of Sciences*, *108*(38), 16050–16055. https://doi.org/10.1073/pnas.1102999108

Cao, X., Kajino-Sakamoto, R., Doss, A., & Aballay, A. (2017). Distinct Roles of Sensory Neurons in Mediating Pathogen Avoidance and Neuropeptide-Dependent Immune Regulation. *Cell Reports*, *21*(6), 1442–1451. https://doi.org/10.1016/j.celrep.2017.10.050

Chen, X., D'Souza, R., & Hong, S.-T. (2013). The role of gut microbiota in the gut-brain axis: current challenges and perspectives. *Protein & Cell*, *4*(6), 403–414. https://doi.org/10.1007/s13238-013-3017-x

Chou, J., Morse, J., Omeis, S., & Venos, E. S. (2005). Escherichia coli C29 Alkaline Phosphatase Enzyme Activity and Protein Level in Exponential and Stationary Phases. *Journal of Experimental Microbiology and Immunology (JEMI)*, *7*, 1–6. https://www.microbiology.ubc.ca/sites/default/files/roles/drupal_ungrad/JEMI/7/7-1.pdf

Cook, S. J., Crouse, C. M., Eviatar Yemini, Hall, D. H., Emmons, S. W., & Hobert, O. (2020). The connectome of the *Caenorhabditis elegans* pharynx. *The Journal of Comparative Neurology*, *528*(16), 2767–2784. https://doi.org/10.1002/cne.24932

Corsi, A. K., Wightman, B., & Chalfie, M. (2015). A Transparent Window into Biology: A Primer on Caenorhabditis elegans. *Genetics*, *200*(2), 387–407. https://doi.org/10.1534/genetics.115.176099

Cresci, G. A. M., & Izzo, K. (2019). Gut Microbiome. *Adult Short Bowel Syndrome*, 45–54. https://doi.org/10.1016/b978-0-12-814330-8.00004-4

Cussotto, S., Sandhu, K. V., Dinan, T. G., & Cryan, J. F. (2018). The Neuroendocrinology of the Microbiota-Gut-Brain Axis: A Behavioural Perspective. *Frontiers in Neuroendocrinology*, *51*, 80–101. https://doi.org/10.1016/j.yfrne.2018.04.002

Ermolaeva, M. A., & Schumacher, B. (2014). Insights from the worm: The C. elegans model for innate immunity. *Seminars in Immunology*, *26*(4), 303–309. https://doi.org/10.1016/j.smim.2014.04.005

Foster, J. A., Rinaman, L., & Cryan, J. F. (2017). Stress & the gut-brain axis: Regulation by the microbiome. *Neurobiology of Stress*, *7*, 124–136. https://doi.org/10.1016/j.ynstr.2017.03.001

Generoso, J. S., Giridharan, V. V., Lee, J., Macedo, D., & Barichello, T. (2020). The role of the microbiota-gut-brain axis in neuropsychiatric disorders. *Brazilian Journal of Psychiatry*. https://doi.org/10.1590/1516-4446-2020-0987

Guinane, C. M., & Cotter, P. D. (2013). Role of the gut microbiota in health and chronic gastrointestinal disease: understanding a hidden metabolic organ. *Therapeutic Advances in Gastroenterology*, *6*(4), 295–308. https://doi.org/10.1177/1756283x13482996

Harrison, X. A., McDevitt, A. D., Dunn, J. C., Griffiths, S., Benvenuto, C., Birtles, R. J., Boubli, J. P., Bown, K. J., Bridson, C., Brooks, D. R., Browett, S. S., Carden, R. F., Chantrey, J., Clever, F., Coscia, I., Witkiewitz, K., Ferry, N., Goodhead, I., Highlands, A., & Hopper, J. (2021). Fungal microbiomes are determined by host phylogeny and exhibit widespread associations with the bacterial microbiome. *The Royal Society*, *288*(1957), 20210552–20210552. https://doi.org/10.1098/rspb.2021.0552

Hermaphrodite - Nervous System - General Overview. (n.d.). Www.wormatlas.org. https://www.wormatlas.org/hermaphrodite/nervous/Neuroframeset.html

Hills, R. D., Pontefract, B. A., Mishcon, H. R., Black, C. A., Sutton, S. C., & Theberge, C. R. (2019). Gut Microbiome: Profound Implications for Diet and Disease. *Nutrients*, *11*(7), 1613. https://www.ncbi.nlm.nih.gov/pmc/articles/PMC6682904/

Holtz, K. M., & Kantrowitz, E. R. (1999). The mechanism of the alkaline phosphatase reaction: insights from NMR, crystallography and site-specific mutagenesis. *FEBS Letters*, *462*(1-2), 7–11. https://doi.org/10.1016/s0014-5793(99)01448-9

Igunnu, A., Osalaye, D. S., Olorunsogo, O. O., Malomo, S. O., & Olorunniji, F. J. (2011). Distinct Metal Ion Requirements for the Phosphomonoesterase and Phosphodiesterase Activities of Calf Intestinal Alkaline Phosphatase. *The Open Biochemistry Journal*, *5*, 67–72. https://doi.org/10.2174/1874091X01105010067

Kantrowitz, E. R. (2011). E. coli Alkaline Phosphatase. *Encyclopedia of Inorganic and Bioinorganic Chemistry*. https://doi.org/10.1002/9781119951438.eibc0479

Kühn, F., Adiliaghdam, F., Cavallaro, P. M., Hamarneh, S. R., Tsurumi, A., Hoda, R. S., Munoz, A. R., Dhole, Y., Ramirez, J. M., Liu, E., Vasan, R., Liu, Y., Samarbafzadeh, E., Nunez, R. A., Farber, M. Z., Chopra, V., Malo, M. S., Rahme, L. G., & Hodin, R. A. (2020). Intestinal alkaline phosphatase targets the gut barrier to prevent aging. *JCI Insight*, *5*(6). https://doi.org/10.1172/jci.insight.134049

Lowe, D., Sanvictores, T., Zubair, M., & John, S. (2023). *Alkaline Phosphatase*. PubMed; StatPearls Publishing. https://www.ncbi.nlm.nih.gov/books/NBK459201/#:~:text=Alkaline%20phosphatases%20(ALPs)%20are%20a

Mayer, E. A., Nance, K., & Chen, S. (2022). The Gut–Brain Axis. *Annual Review of Medicine*, *73*(1), 439–453. https://doi.org/10.1146/annurev-med-042320-014032

Mukherji, A., Kobiita, A., Ye, T., & Chambon, P. (2013). Homeostasis in Intestinal Epithelium Is Orchestrated by the Circadian Clock and Microbiota Cues Transduced by TLRs. *Cell*, *153*(4), 812–827. https://doi.org/10.1016/j.cell.2013.04.020

Narisawa, S., Hasegawa, H., Watanabe, K., & Millán, J. L. (1994). Stage-specific expression of alkaline phosphatase during neural development in the mouse. *Developmental Dynamics*, *201*(3), 227–235. https://doi.org/10.1002/aja.1002010306

Narisawa, S., Huang, L., Iwasaki, A., Hasegawa, H., Alpers, D. H., & MillánJ. L. (2003). Accelerated Fat Absorption in Intestinal Alkaline Phosphatase Knockout Mice. *Molecular and Cellular Biology*, *23*(21), 7525–7530. https://doi.org/10.1128/mcb.23.21.7525-7530.2003

Reddy, K. C., Andersen, E. C., Leonid Kruglyak, & Kim, D. H. (2009). A Polymorphism in *npr-1* Is a Behavioral Determinant of Pathogen Susceptibility in *C. elegans*. *Science*, *323*(5912), 382–384. https://doi.org/10.1126/science.1166527

Sharma, U., Pal, D., & Prasad, R. (2013). Alkaline Phosphatase: An Overview. *Indian Journal of Clinical Biochemistry*, *29*(3), 269–278. https://doi.org/10.1007/s12291-013-0408-y

Shtonda BB, Avery L. Dietary choice behavior in Caenorhabditis elegans. J Exp Biol. 2006 Jan;209(Pt 1):89-102. doi: 10.1242/jeb.01955. PMID: 16354781; PMCID: PMC1352325.

Singh, J., & Aballay, A. (2020). Neural control of behavioral and molecular defenses in C. elegans. *Current Opinion in Neurobiology*, *62*, 34–40. https://doi.org/10.1016/j.conb.2019.10.012

Sudo, N., Chida, Y., Aiba, Y., Sonoda, J., Oyama, N., Yu, X.-N., Kubo, C., & Koga, Y. (2004). Postnatal microbial colonization programs the hypothalamic-pituitary-adrenal system for stress response in mice. *The Journal of Physiology*, *558*(1), 263–275. https://doi.org/10.1113/jphysiol.2004.063388

Vimalraj, S. (2020). Alkaline phosphatase: Structure, expression and its function in bone mineralization. *Gene*, *754*(754), 144855. https://doi.org/10.1016/j.gene.2020.144855

WormBase : Nematode Information Resource. (2012). Wormbase.org. https://wormbase.org/#012-34-5

Zalatan, J. G., Fenn, T. D., & Herschlag, D. (2008). Comparative Enzymology in the Alkaline Phosphatase Superfamily to Determine the Catalytic Role of an Active-Site Metal Ion. *Journal of Molecular Biology*, *384*(5), 1174–1189. https://doi.org/10.1016/j.jmb.2008.09.059

Appendix

a. M9 Buffer

Autoclaved together:

- 3g Na_2HPO_4
- 1.5g KH_2PO_4
- 2.5g NaCl
- 500 mL sterile H_2O

Autoclaved separately, then added:

- 0.5 mL 1M $MgSO_4$ solution
    - 12.32g $MgSO_4 \cdot 7H_2O$
    - 50mL sterile H_2O

b. Nematode Growth Medium (NGM)

Autoclaved together:

- 2.4g (0.3%) NaCl
- 16g (1.2%) Agar
- 2g Peptone
- 280 mL DI H_2O

Autoclaved separately, then added:

- 20mL KPO_4 Buffer
    - 21.66g KH_2PO_4
    - 7.12g K_2HPO_4
    - 200mL DI H_2O
- 0.8mL $MgSO_4$ solution
    - 12.32g $MgSO_4 \cdot 7H_2O$
    - 50mL DI H_2O
- 0.8ml $CaCl_2$ solution
    - 5.55g $CaCl_2$
    - 50mL DI H_2O
- 0.8mL 0.5% cholesterol solution
- 0.25g Cholesterol
- 50mL Ethanol (EtOH)

c. Yeast Extract Peptone Dextrose (YPD) Media

Autoclaved together:

- 8g (1%) Yeast Extract
- 16g (2%) Peptone
- 750mL DI H_2O

Autoclaved separately, then added:

- 50mL 2% Glucose solution
    - 16g (2%) Dextrose
    - 50mL DI H2O

d. Lysogeny Broth (LB)

- 8g (1%) Tryptone
- 4g (0.5%) Yeast Extract
- 4g (0.5%) NaCl
- 800mL DI H2O

e. cDNA Master Mix

For 1x solution, prepared on ice:

- 2 uL 10X RT buffer
- 0.8 uL 25X dNTP mix
- 2 uL 10X RT Random primers
- 3.2 uL Nuclease-free water
- 1 uL MultiScribe Rev Transcriptase (half)
- 1 uL Nuclease-free water (half)

f. qPCR Master Mix

For primer mix (2.5 uM): # of wells + 10% = total volume

i.e 16 wells + 10% = ~18

- 4.5 uL Forward 10uM
- 4.5 uL Reverse 10 uM
- 9 uL Nuclease-free water

Total = 18 uL

For each primer set:

For 1X solution:	For 16 samples:
- 5 uL iTaq Sybr green mix	90 uL
- 1 uL primer mix	18 uL
- 2 mL Nuclease-free water	36 uL

g. Relative Quantification

Key:

- Calibrator samples: OP50
- Test samples: F15
- Reference Gene: CDC 42

- Target Genes: daf7, pmk1, flp18, flp21, npr1

ΔCt (calibrator samples) = Ct (target gene in calibrator) - Ct (reference gene in calibrator)
ΔCt (test samples) = Ct (target gene in test) - Ct (reference gene in test)

ΔΔCt = ΔCt (test samples) - ΔCt (calibrator samples)

RQ = $2^{-\Delta\Delta Ct}$